


## Article

# Chemical Profiling of Kaliziri Injection and Quantification of Six Caffeoyl Quinic Acids in Beagle Plasma by LC-MS/MS

Changhua Liu<sup>1,2</sup>, Atikanmu Wahefu<sup>1,2</sup>, Xueying Lu<sup>1</sup>, Rahima Abdulla<sup>1</sup>, Jun Dou<sup>1</sup>, Haiqing Zhao<sup>1</sup>, Haji Akber Aisa<sup>1</sup> , Xueleixin<sup>1,\*</sup> and Yongqiang Liu<sup>1,\*</sup>

- <sup>1</sup> State Key Laboratory Basis of Xinjiang Indigenous Medicinal Plants Resource Utilization, Key Laboratory of Plant Resources and Chemistry of Arid Zone, Xinjiang Technical Institute of Physics and Chemistry, Chinese Academy of Sciences, Urumqi 830011, China; wowlch22045@163.com (C.L.); atikanmu18@mails.ucas.ac.cn (A.W.); xueyinglu@ms.xjb.ac.cn (X.L.); rahima@ms.xjb.ac.cn (R.A.); doujun@ms.xjb.ac.cn (J.D.); haiqing\_zhq@ms.xjb.ac.cn (H.Z.); haji@ms.xjb.ac.cn (H.A.A.)
- <sup>2</sup> University of Chinese Academy of Sciences, Beijing 100049, China
- \* Correspondence: xinxl@ms.xjb.ac.cn (X.X.); liuyq@ms.xjb.ac.cn (Y.L.)

**Abstract:** Vitiligo is a stubborn multifactorial skin disease with a prevalence of approximately 1% in the global population. Kaliziri, the seeds of *Vernonia anthelmintica* (L.) Willd., is a well-known traditional Uyghur medicine for the treatment of vitiligo. Kaliziri injections is a Chinese-marketed treatment approved by the China Food and Drug Administration for the treatment of vitiligo. The significant effects of Kaliziri injection have been thoroughly studied. However, chemical components studies and plasma quantification studies are lacking for Kaliziri injection. Ultra-high-performance liquid chromatography coupled with hybrid quadrupole orbitrap mass spectrometry was employed to comprehensively characterize the caffeoyl quinic acid derivatives present in Kaliziri injection. Based on accurate mass measurements, key fragmental ions and comparisons with reference standards, 60 caffeoyl quinic acid derivatives were identified in Kaliziri injections, including caffeoyl quinic acids, coumaroyl caffeoyl quinic acids, dicaffeoyl quinic acids, feruloyl caffeoyl quinic acids, and dicaffeoyl quinic acid hexosides. Moreover, an HPLC-MS/MS method was developed and validated for the quantitative analysis of 5-caffeoyl quinic acid, 4-caffeoyl quinic acid, 1,3-dicaffeoyl quinic acid, 3,4-dicaffeoyl quinic acid, 3,5-dicaffeoyl quinic acid and 4,5-dicaffeoyl quinic acid in beagle plasma. The quantitative HPLC-MS/MS method was applied to quantify these six major caffeoyl quinic acids in beagle plasma after the subcutaneous administration of Kaliziri injection. All of the six analytes reached their peak plasma of concentrations within 30 min.

**Keywords:** Kaliziri injection; caffeoyl quinic acid derivatives; UHPLC-Q-Orbitrap-MS; beagle plasma; tandem mass spectrometry; quantitative analysis



**Citation:** Liu, C.; Wahefu, A.; Lu, X.; Abdulla, R.; Dou, J.; Zhao, H.; Aisa, H.A.; Xin, X.; Liu, Y. Chemical Profiling of Kaliziri Injection and Quantification of Six Caffeoyl Quinic Acids in Beagle Plasma by LC-MS/MS. *Pharmaceuticals* **2022**, *15*, 663. <https://doi.org/10.3390/ph15060663>

Academic Editor: Daniela De Vita

Received: 27 April 2022

Accepted: 24 May 2022

Published: 25 May 2022

**Publisher's Note:** MDPI stays neutral with regard to jurisdictional claims in published maps and institutional affiliations.



**Copyright:** © 2022 by the authors. Licensee MDPI, Basel, Switzerland. This article is an open access article distributed under the terms and conditions of the Creative Commons Attribution (CC BY) license (<https://creativecommons.org/licenses/by/4.0/>).

## 1. Introduction

Vitiligo, caused by the loss of the function of melanocytes and melanin in skin and hair, is an autoimmune disease characterized by the appearance of white spots, with an estimated prevalence of approximately 1% in the global population [1,2]. Clinical and epidemiological investigations have shown that vitiligo is a complex multifactorial disease [3].

Contemporary treatment strategies for vitiligo include phototherapy, local or systemic immunosuppressive agents, and surgical treatment [4]. However, these treatments can only prevent the progression of the disease and promote the re-coloring of depigmented areas, but cannot completely cure vitiligo. Therefore, vitiligo's recurrence has grave impacts on the physical health, quality of life and social communication of these patients resulting in some psychological disorders, such as the development of an inferiority complex and social isolation [5,6].

The seeds of *Vernonia anthelmintica* (L.) Willd. (Quchong Banjiuju) are called Kaliziri in traditional Uyghur medicine, and have traditionally been used for the treatment of

vitiligo [7]. In a prior phytochemical investigation, we reported the isolation and structure elucidation of sesquiterpene components in petroleum ether extracts of Kaliziri (though by NMR spectroscopy). In particular, the 21 newly identified vernodalidimers are rare elemanolide type dimers [8]. The mechanism of Kaliziri extract against vitiligo has been studied from enzymology, cell, and molecule aspects. The results show that Kaliziri extract can directly activate tyrosinase activity in B16 melanocytes and promote the melanin content and tyrosinase activity of B16 melanocytes; RT-PCR and western blot experiments further revealed that it can promote the upregulation of several genes and proteins closely associated with melanin synthesis in B16 melanoma cells, including MITF, TYR, TRP1, and TRP2. It was also found that it can stimulate melanin production in B16 cells by activating the MAPK and cAMP/PKA signaling pathway [7,9–14].

Kaliziri injection (KZI) is a Chinese-marketed treatment approved by the China Food and Drug Administration with an approval number of Z20063652. KZI is a preparation of aqueous Kaliziri extract and is used for the treatment of vitiligo. It is widely used in clinical combined treatment, and the effect is significant. Clinically, 308 nm excimer light combined with KZI is used to treat vitiligo. Compared with a control group, the effective rate of a treatment group was 26.8% higher, demonstrating a significant curative effect and high safety [15]. KZI combined with a vitiligo pill also had a significant effect on vitiligo. After 12 weeks of treatment, the effective rate of a control group was 41.2%, whereas that of a treatment group was 73.5% [16]. In addition, KZI can significantly inhibit the proliferation of T cells and B cells significantly in mice, which is related to the dosage of the injection. At the same time, KZI can activate tyrosinase activity in mice [17].

However, the chemical components of KZI have not yet been investigated. Additionally, the plasma quantification of key components has not been studied. Tandem mass spectrometry can powerfully characterize chemical components in herbs and plants [18–22]. Ultra-high-performance liquid chromatography coupled with quadrupole orbitrap mass spectrometry (UHPLC-Q-Orbitrap-MS) hybridizes the high mass resolution of orbitrap and the excellent selectivity of the quadrupole [23]. Herein, UHPLC-Q-Orbitrap-MS was employed to comprehensively identify caffeoyl quinic acid derivatives present in KZI. Moreover, an HPLC-MS/MS method was developed for the simultaneous quantitative analysis of six caffeoyl quinic acids in beagle plasma after the subcutaneous injection of Kaliziri.

## 2. Results and Discussion

### 2.1. The Identification of Caffeoyl Quinic Acid Derivatives in KZI by UHPLC-Q-Orbitrap-MS

The UHPLC-Q-Orbitrap-MS total ion chromatogram (TIC) of KZI is shown in Figure 1. Based on the accurate mass measurements, the key fragmental ions and the comparison with reference standards, 60 caffeoyl quinic acid derivatives were identified in KZI. The results are shown in Table 1.

The typical fragmental ions of caffeoyl quinic acid derivatives were preliminarily determined by standards using UHPLC-Q-Orbitrap-MS. Typically, fragmental ions at  $m/z$  191 ( $C_7H_{11}O_6^-$ ) correspond to [quinic acid-H] $^-$ ,  $m/z$  173 ( $C_7H_9O_5^-$ ) correspond to [quinic acid-H-H<sub>2</sub>O] $^-$ , and  $m/z$  179 ( $C_9H_7O_4^-$ ) corresponding to [caffeic acid-H] $^-$ . The fragment pathway of 4,5-dicaffeoyl quinic acid is shown in Figure 2.

Compounds 2, 4, 7, and 8 exhibited the [M-H] $^-$  ions at  $m/z$  353, with a molecular formula of  $C_{16}H_{18}O_9$ . In the MS/MS spectra, they revealed diagnostic [quinic acid-H] $^-$  ions at  $m/z$  191 [M-H-162] $^-$  as well as a diagnostic loss of 162 Da ( $C_9H_6O_3$ ) for a caffeoyl moiety, suggesting that these compounds were caffeoyl quinic acids (CQAs). From comparisons of the retention time, high-resolution MS data, and MS/MS spectra data with those of authentic standards, compounds 4, 7, and 8 were identified as 3-caffeoyl quinic acid (3-CQA), 5-caffeoyl quinic acid (5-CQA) and 4-caffeoyl quinic acid (4-CQA). Compounds 6, 12 and 13 gave [M-H] $^-$  ions at  $m/z$  337, with a molecular formula of  $C_{16}H_{18}O_8$ . In the MS/MS spectra, their diagnostic [quinic acid-H] $^-$  ion at  $m/z$  191 [M-H-162] $^-$  as well as diagnostic loss of 146 Da ( $C_9H_6O_2$ ) for a coumaroyl moiety suggesting that these

compounds were coumaroyl quinic acids. Compounds **17** and **18** exhibited  $[M-H]^-$  ions at  $m/z$  367, with molecular formula of  $C_{17}H_{20}O_9$ . In the MS/MS spectra, their diagnostic  $[quinic\ acid-H]^-$  ion at  $m/z$  191  $[M-H-162]^-$  as well as the diagnostic loss of 176 Da ( $C_{10}H_8O_3$ ) for a feruloyl moiety suggested that compounds **17** and **18** were feruloyl quinic acids (FQAs). Compounds **10**, **14** and **16** exhibited the same  $[M-H]^-$  ions at  $m/z$  399, with a molecular formula of  $C_{18}H_{24}O_{10}$ . Their fragmental ions at  $m/z$  353 ( $[CQA-H]^-$  and  $[M-C_2H_6O-H]^-$ ), as well as diagnostic ions at  $m/z$  179 ( $[caffeic\ acid-H]^-$ ), indicated that these compounds were caffeoyl quinic acid ethyl esters.

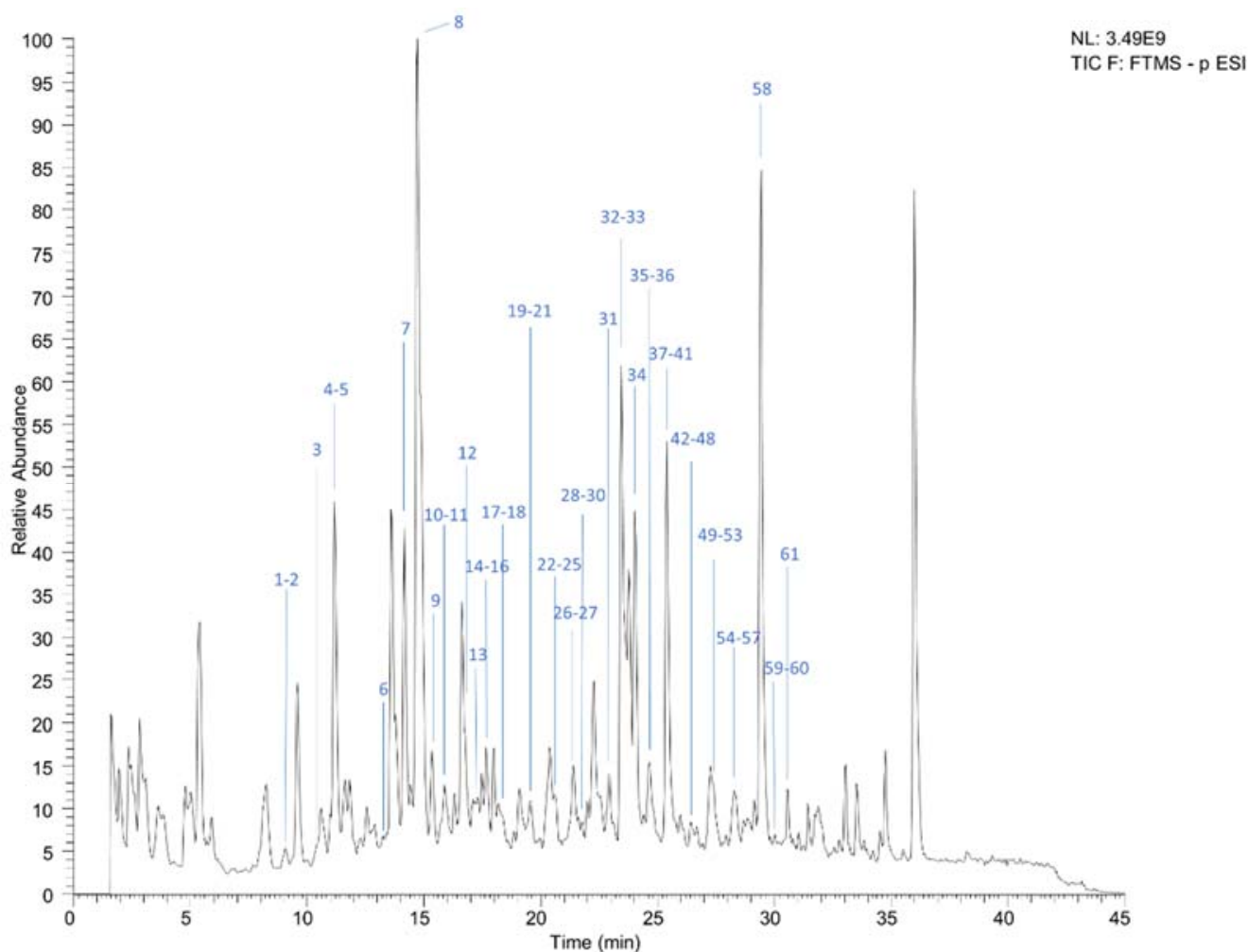


**Figure 1.** The total ion chromatogram of KZI by UHPLC-Q-Orbitrap-MS.

Compounds **15**, **33**, **34** and **37** exhibited same  $[M-H]^-$  ions at  $m/z$  515, with a molecular formula of  $C_{25}H_{24}O_{12}$ . In the MS/MS spectra, they exhibited a diagnostic  $[CQA-H]^-$  ion at  $m/z$  353  $[M-H-162]^-$  and  $[quinic\ acid-H]^-$  ion at  $m/z$  191  $[M-H-162-162]^-$  suggesting that these compounds were dicaffeoyl quinic acids (diCQAs). From comparison of the retention time, high-resolution MS data, and MS/MS spectra data with those of authentic standards, compounds **15**, **33**, **34** and **37** were identified as 1,3-dicaffeoyl quinic acid (1,3-diCQA), 3,4-dicaffeoyl quinic acid (3,4-diCQA), 3,5-dicaffeoyl quinic acid (3,5-diCQA) and 4,5-dicaffeoyl quinic acid (4,5-diCQA), respectively. Compounds **22**, **27**, **40**, **41**, **43**, **45**, **53** and **54** exhibited the same  $[M-H]^-$  ions at  $m/z$  499, with molecular a formula of  $C_{25}H_{24}O_{11}$ . Their diagnostic fragmental ions at  $m/z$  353  $[CQA-H]^-$  or  $m/z$  337  $[CoQA-H]^-$ , diagnostic ions at  $m/z$  179  $[caffeic\ acid-H]^-$  or  $m/z$  163  $[coumaric\ acid-H]^-$  and diagnostic ions at  $m/z$  191  $[quinic\ acid-H]^-$  indicated that these compounds were coumaroyl caffeoyl quinic acids (CoCQAs). Compounds **42**, **46**, **49**, **51**, **55** and **56** exhibited the same  $[M-H]^-$  ions at  $m/z$  529, with a molecular formula of  $C_{26}H_{26}O_{12}$ . Their diagnostic fragmental ions at  $m/z$

353 [CQA-H]<sup>-</sup> or *m/z* 367 [FQA-H]<sup>-</sup>, diagnostic ions at *m/z* 179 [caffeic acid-H]<sup>-</sup> or *m/z* 193 [ferulic acid-H]<sup>-</sup> and diagnostic ions at *m/z* 191 [quinic acid-H]<sup>-</sup> indicated that these compounds were feruloyl caffeoyl quinic acids. Compounds **9**, **24**, **26** and **31** exhibited the same [M-H]<sup>-</sup> ions at *m/z* 489, with a molecular formula of C<sub>23</sub>H<sub>23</sub>O<sub>12</sub>. Their diagnostic fragmental ions at *m/z* 179 [caffeic acid-H]<sup>-</sup> or *m/z* 153 [dihydroxybenzoic acid-H]<sup>-</sup>, diagnostic ions at *m/z* 353 [CQA-H]<sup>-</sup> or *m/z* 327 [dihydroxybenzoyl quinic acid-H]<sup>-</sup> and diagnostic ions at *m/z* 191 [quinic acid-H]<sup>-</sup> indicated that these compounds were dihydroxybenzoyl caffeoyl quinic acids. Compounds **35**, **36**, **38**, **39**, **44**, **47**, **48**, **50** and **52** exhibited the same [M-H]<sup>-</sup> ions at *m/z* 561, with a molecular formula of C<sub>27</sub>H<sub>30</sub>O<sub>13</sub>. In the MS/MS spectra, they exhibited diagnostic ions at *m/z* 515 [diCQA-H]<sup>-</sup>, *m/z* 353 [CQA-H]<sup>-</sup>, *m/z* 191 [quinic acid-H]<sup>-</sup> and *m/z* 179 [caffeic acid-H]<sup>-</sup>, which indicated that they were derivatives of diCQA. Furthermore, the daughter ions at *m/z* 515 [M-C<sub>2</sub>H<sub>6</sub>O-H]<sup>-</sup>, *m/z* 399 [M-caffeoyl-H]<sup>-</sup> and *m/z* 353 [M-caffeoyl-C<sub>2</sub>H<sub>6</sub>O-H]<sup>-</sup> suggested that compounds **35**, **36**, **38**, **39**, **44**, **47**, **48**, **50** and **52** were dicaffeoyl quinic acid ethyl esters. The structures of substituents connect to quinic acid are shown in Figure 3.

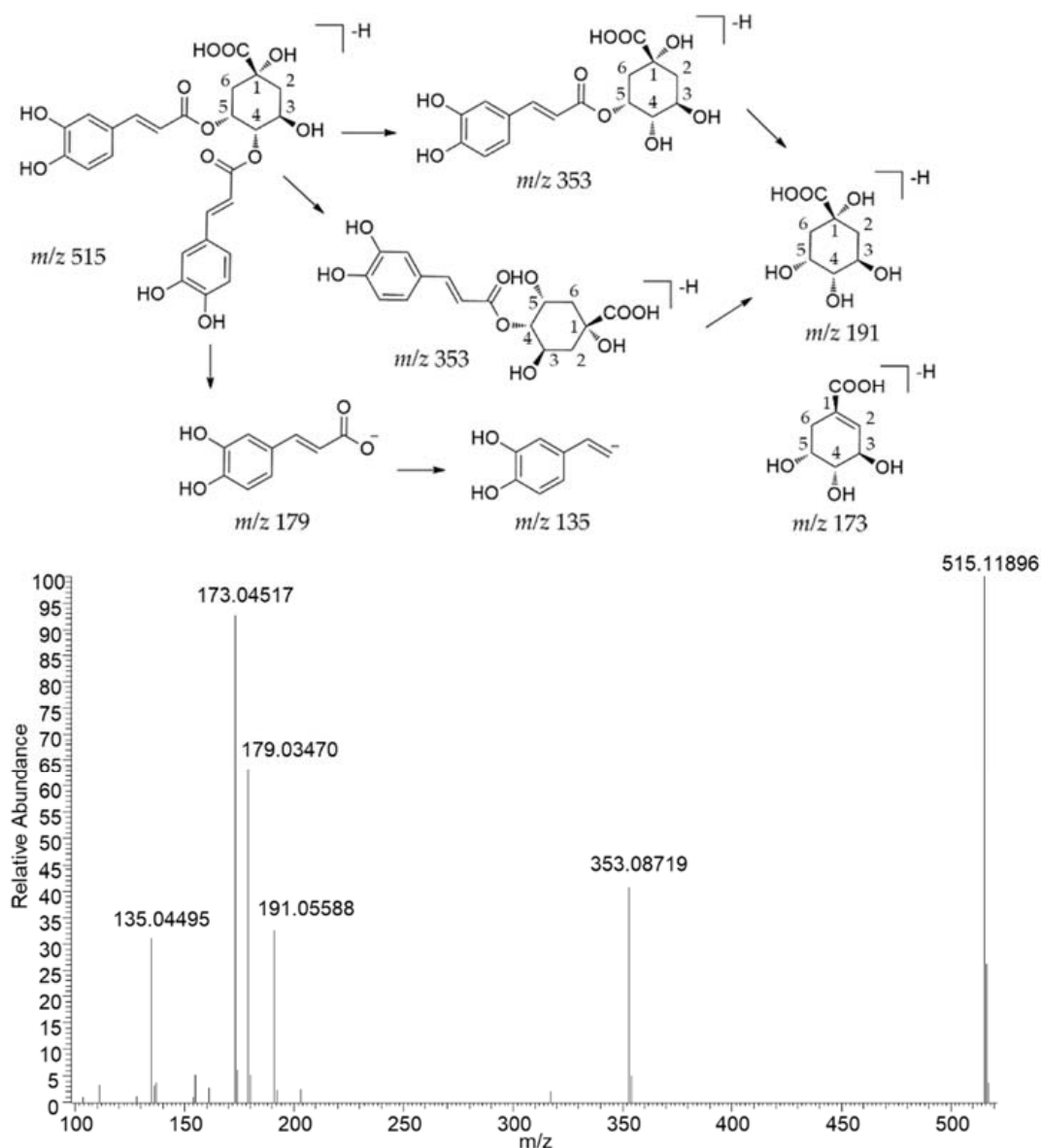


Figure 2. The fragment pathway of 4,5-dicaffeoyl quinic acid.

**Table 1.** Caffeoyl quinic acid derivative characterization of KZI by UHPLC-Q-Orbitrap-MS.

No.	$t_R$ (min)	Molecular Formula	[M-H] <sup>-</sup>	Major and Important MS <sup>2</sup> Ions	Identification	Error (ppm)
1	9.22	C <sub>28</sub> H <sub>38</sub> O <sub>19</sub>	677.19519	515, 353, 341, 191, 179, 173, 161, 135	CQA hexosyl hexoside-a	4.19
2	9.32	C <sub>16</sub> H <sub>18</sub> O <sub>9</sub>	353.08719	191	CQA	1.36
3	10.13	C <sub>28</sub> H <sub>38</sub> O <sub>19</sub>	677.19562	515, 353, 323, 191, 179, 173, 161, 135	CQA hexosyl hexoside-b	4.82
4	11.18	C <sub>16</sub> H <sub>18</sub> O <sub>9</sub>	353.08566	191, 179, 135	3-CQA *	-2.90
5	11.51	C <sub>28</sub> H <sub>38</sub> O <sub>19</sub>	677.19537	515, 353, 341, 179, 173, 135	CQA hexosyl hexoside-c	4.46
6	13.28	C <sub>16</sub> H <sub>18</sub> O <sub>8</sub>	337.09326	191, 173, 163, 119	CoQA-a	4.35
7	14.15	C <sub>16</sub> H <sub>18</sub> O <sub>9</sub>	353.08627	191	5-CQA *	-1.20
8	14.86	C <sub>16</sub> H <sub>18</sub> O <sub>9</sub>	353.08517	191, 179, 173, 135	4-CQA *	-4.30
9	15.47	C <sub>23</sub> H <sub>22</sub> O <sub>12</sub>	489.10510	353, 335, 191, 179, 161, 135, 109	dihydroxybenzoyl CQA-a	4.80
10	15.81	C <sub>18</sub> H <sub>24</sub> O <sub>10</sub>	399.13062	353, 191, 179, 135	CQA ethyl ester-a	5.12
11	16.07	C <sub>34</sub> H <sub>30</sub> O <sub>16</sub>	693.14832	531, 353, 339, 313, 295, 269, 229, 191, 173, 159, 109	Trihydroxycinnamoyl diCQA-a	4.77
12	16.79	C <sub>16</sub> H <sub>18</sub> O <sub>8</sub>	337.09351	191, 173, 163, 119	CoQA-b	5.07
13	17.11	C <sub>16</sub> H <sub>18</sub> O <sub>8</sub>	337.09311	191, 173, 163, 137, 119	CoQA-c	3.90
14	17.54	C <sub>18</sub> H <sub>24</sub> O <sub>10</sub>	399.13055	353, 191, 179, 135	CQA ester-b	4.96
15	17.63	C <sub>25</sub> H <sub>24</sub> O <sub>12</sub>	515.12024	353, 191, 179, 135	1,3-diCQA *	3.56
16	17.73	C <sub>18</sub> H <sub>24</sub> O <sub>10</sub>	399.13043	353, 191, 179, 135	CQA ethyl ester-c	4.66
17	18.32	C <sub>17</sub> H <sub>20</sub> O <sub>9</sub>	367.10413	191, 134	FQA-a	4.81
18	18.42	C <sub>17</sub> H <sub>20</sub> O <sub>9</sub>	367.10413	193, 191, 173, 155, 134	FQA-b	4.81
19	19.19	C <sub>34</sub> H <sub>30</sub> O <sub>16</sub>	693.14783	531, 353, 339, 313, 295, 269, 229, 191, 179, 173, 159, 109	Trihydroxycinnamoyl diCQA-b	4.06
20	19.33	C <sub>34</sub> H <sub>30</sub> O <sub>16</sub>	693.14789	531, 353, 339, 313, 295, 269, 229, 191, 179, 173, 159, 109	Trihydroxycinnamoyl diCQA-c	4.15
21	19.52	C <sub>34</sub> H <sub>30</sub> O <sub>16</sub>	693.14801	531, 353, 339, 295, 269, 229, 191, 179, 173, 159, 135, 109	Trihydroxycinnamoyl diCQA-d	4.33
22	20.39	C <sub>25</sub> H <sub>24</sub> O <sub>11</sub>	499.12573	353, 335, 191, 179, 161, 135	CoCQA-a	4.50
23	20.42	C <sub>34</sub> H <sub>30</sub> O <sub>16</sub>	693.14764	531, 353, 339, 295, 267, 229, 191, 179, 173, 159, 135, 109	Trihydroxycinnamoyl diCQA-e	3.80
24	20.55	C <sub>23</sub> H <sub>22</sub> O <sub>12</sub>	489.10468	353, 335, 327, 309, 191, 179, 173, 161, 153, 135, 109	dihydroxybenzoyl CQA-b	3.93
25	20.61	C <sub>34</sub> H <sub>30</sub> O <sub>16</sub>	693.14752	531, 353, 339, 313, 295, 269, 229, 191, 179, 173, 159, 109	Trihydroxycinnamoyl diCQA-f	3.62
26	21.05	C <sub>23</sub> H <sub>22</sub> O <sub>12</sub>	489.10498	327, 191, 179, 153, 109	dihydroxybenzoyl CQA-c	4.56
27	21.11	C <sub>25</sub> H <sub>24</sub> O <sub>11</sub>	499.12570	337, 191, 163, 119	CoCQA-b	4.44
28	21.43	C <sub>31</sub> H <sub>34</sub> O <sub>17</sub>	677.17371	515, 353, 323, 191, 179, 173, 161, 135	diCQA hexoside-a	3.66
29	21.79	C <sub>31</sub> H <sub>34</sub> O <sub>17</sub>	677.17450	515, 353, 323, 191, 179, 173, 161, 135	diCQA hexoside-b	4.83
30	22.26	C <sub>31</sub> H <sub>34</sub> O <sub>17</sub>	677.17383	515, 353, 323, 191, 179, 173, 161, 135	diCQA hexoside-c	3.84
31	22.85	C <sub>23</sub> H <sub>22</sub> O <sub>12</sub>	489.10477	327, 191, 173, 153, 109	dihydroxybenzoyl CQA-d	4.12
32	23.31	C <sub>31</sub> H <sub>34</sub> O <sub>17</sub>	677.17444	515, 353, 323, 191, 179, 173, 161, 135	diCQA hexoside-d	4.75
33	23.50	C <sub>25</sub> H <sub>24</sub> O <sub>12</sub>	515.11975	353, 335, 191, 179, 173, 135	3,4-diCQA *	2.62
34	24.07	C <sub>25</sub> H <sub>24</sub> O <sub>12</sub>	515.12006	353, 191, 179, 135	3,5-diCQA *	3.21
35	24.76	C <sub>27</sub> H <sub>30</sub> O <sub>13</sub>	561.16260	515, 399, 353, 191, 179, 173, 161, 135	diCQA ethyl ester-a	4.15

Table 1. Cont.

No.	$t_R$ (min)	Molecular Formula	$[M-H]^-$	Major and Important MS <sup>2</sup> Ions	Identification	Error (ppm)
36	24.99	C <sub>27</sub> H <sub>30</sub> O <sub>13</sub>	561.16266	515, 399, 353, 191, 179, 173, 161, 135	diCQA ethyl ester-b	4.26
37	25.42	C <sub>25</sub> H <sub>24</sub> O <sub>12</sub>	515.11987	353, 191, 179, 173, 135	4,5-diCQA *	2.85
38	25.51	C <sub>27</sub> H <sub>30</sub> O <sub>13</sub>	561.16193	515, 399, 353, 335, 191, 179, 173, 161, 135	diCQA ethyl ester-c	2.96
39	25.74	C <sub>27</sub> H <sub>30</sub> O <sub>13</sub>	561.16241	515, 399, 353, 335, 191, 179, 173, 161, 135	diCQA ethyl ester-d	3.83
40	25.77	C <sub>25</sub> H <sub>24</sub> O <sub>11</sub>	499.12561	353, 337, 335, 319, 191, 179, 173, 163, 135, 119	CoCQA-c	4.25
41	26.14	C <sub>25</sub> H <sub>24</sub> O <sub>11</sub>	499.12567	353, 337, 319, 191, 179, 173, 163, 119	CoCQA-d	4.37
42	26.31	C <sub>26</sub> H <sub>26</sub> O <sub>12</sub>	529.13617	365, 335, 193, 191, 179, 175, 173, 161, 135, 134	FCQA-a	4.00
43	26.41	C <sub>25</sub> H <sub>24</sub> O <sub>11</sub>	499.12570	337, 191, 173, 163, 119	CoCQA-e	4.44
44	26.41	C <sub>27</sub> H <sub>30</sub> O <sub>13</sub>	561.16266	499, 414, 399, 353, 191, 179, 173, 161, 135	diCQA ethyl ester-e	4.26
45	26.64	C <sub>25</sub> H <sub>24</sub> O <sub>11</sub>	499.12564	353, 337, 191, 179, 173, 135	CoCQA-f	4.31
46	26.81	C <sub>26</sub> H <sub>26</sub> O <sub>12</sub>	529.13617	367, 335, 193, 173, 161, 134	FCQA-b	4.00
47	26.85	C <sub>27</sub> H <sub>30</sub> O <sub>13</sub>	561.16272	515, 441, 399, 353, 191, 179, 173, 135	diCQA ethyl ester-f	4.37
48	27.28	C <sub>27</sub> H <sub>30</sub> O <sub>13</sub>	561.16254	515, 399, 353, 191, 179, 173, 135	diCQA ethyl ester-g	4.04
49	27.41	C <sub>26</sub> H <sub>26</sub> O <sub>12</sub>	529.13599	367, 193, 179, 134	FCQA-c	3.65
50	27.47	C <sub>27</sub> H <sub>30</sub> O <sub>13</sub>	561.16260	515, 399, 353, 191, 179, 173, 161, 135	diCQA ethyl ester-h	4.15
51	27.61	C <sub>26</sub> H <sub>26</sub> O <sub>12</sub>	529.13629	367, 353, 191, 179, 135	FCQA-d	4.23
52	27.61	C <sub>27</sub> H <sub>30</sub> O <sub>13</sub>	561.16278	515, 399, 353, 351, 191, 179, 173, 135	diCQA ethyl ester-i	4.48
53	27.81	C <sub>25</sub> H <sub>24</sub> O <sub>11</sub>	499.12567	337, 191, 173, 163, 119	CoCQA-g	4.37
54	27.98	C <sub>25</sub> H <sub>24</sub> O <sub>11</sub>	499.12576	353, 337, 191, 179, 173, 163, 135	CoCQA-h	4.56
55	28.19	C <sub>26</sub> H <sub>26</sub> O <sub>12</sub>	529.13593	367, 183, 173, 134	FCQA-e	3.54
56	28.38	C <sub>26</sub> H <sub>26</sub> O <sub>12</sub>	529.13562	367, 353, 335, 191, 179, 173, 135	FCQA-f	2.96
57	29.52	C <sub>34</sub> H <sub>30</sub> O <sub>15</sub>	677.15283	515, 353, 335, 191, 179, 173, 161, 135	triCQA	4.04
58	30.02	C <sub>35</sub> H <sub>34</sub> O <sub>15</sub>	693.18433	531, 513, 353, 335, 191, 179, 177, 173, 161, 135, 133	Hydroferuoyl diCQA	4.23
59	30.19	C <sub>35</sub> H <sub>34</sub> O <sub>15</sub>	693.18445	531, 335, 191, 179, 177, 173, 161, 135, 133	Hydroferuoyl diCQA	4.40
60	30.58	C <sub>35</sub> H <sub>34</sub> O <sub>15</sub>	693.18408	531, 353, 191, 179, 173, 135	Hydroferuoyl diCQA	3.87

\* Identified by comparing with reference standard: CQA, caffeoyl quinic acid; CoQA, coumaroyl quinic acid; diCQA, dicaffeoyl quinic acid; FQA, feruloyl quinic acid; FCQA, feruloyl caffeoyl quinic acid; CoCQA, coumaroyl caffeoyl quinic acid; triCQA, tricaffeoyl quinic acid.

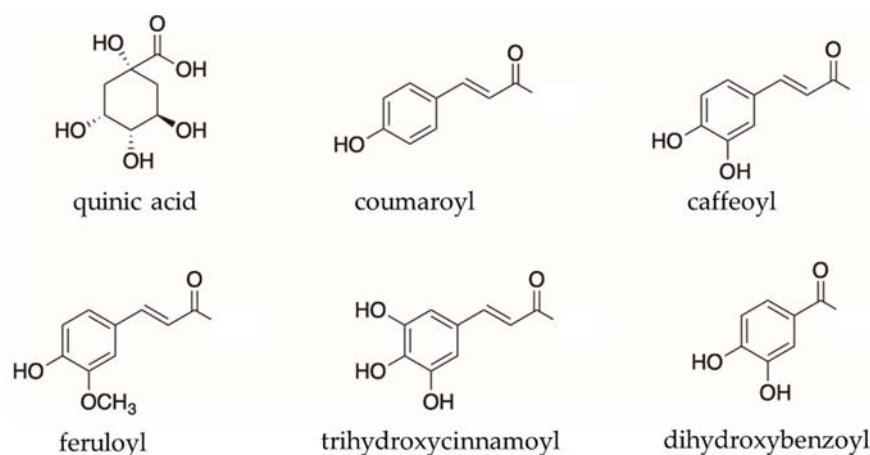


**Figure 3.** Selected structures of substituents associated with quinic acid.

Compound **57** exhibited  $[M-H]^-$  ions at  $m/z$  677, with a molecular formula of  $C_{34}H_{30}O_{15}$ . Its diagnostic fragmental ions at  $m/z$  515 ( $[diCQA-H]^-$ ,  $[M\text{-caffeic acid-H}]^-$ ),  $m/z$  353  $[CQA-H]^-$ ,  $m/z$  191  $[quinic\ acid-H]^-$  and  $m/z$  179  $[caffeic\ acid-H]^-$  indicated that compound **57** was tricaffeoyl quinic acid. Compounds **10**, **19**, **20**, **21**, **23** and **25** exhibited the same  $[M-H]^-$  ions at  $m/z$  693, with a molecular formula of  $C_{34}H_{30}O_{16}$ , one oxygen more than compound **57**. In the MS/MS spectra, their diagnostic ions at  $m/z$  353  $[CQA-H]^-$ ,  $m/z$  191  $[quinic\ acid-H]^-$  and  $m/z$  179  $[caffeic\ acid-H]^-$  indicated that they were derivatives of CQA. Moreover, their fragmental ions at  $m/z$  531  $[M\text{-caffeoyl-H}]^-$  and  $m/z$  353  $[M\text{-caffeoyl-trihydroxycinnamoyl-H}]^-$  suggested that these compounds were trihydroxycinnamoyl-dicafeoyl quinic acids.

Compounds **28**, **29**, **30** and **32** exhibited the same  $[M-H]^-$  ions at  $m/z$  677.17371, with a molecular formula of  $C_{31}H_{34}O_{17}$ . In the MS/MS spectra, their diagnostic ions at  $m/z$  353  $[CQA-H]^-$ ,  $m/z$  191  $[quinic\ acid-H]^-$  and  $m/z$  179  $[caffeic\ acid-H]^-$  indicated that they were derivatives of CQA. Meanwhile, the daughter ions at  $m/z$  515 ( $[diCQA-H]^-$ ,  $[M\text{-}C_6H_{10}O_5-H]^-$ ) indicated the existence of a hexosyl group and another caffeoyl group. Thus, compounds **28**, **29**, **30**, and **32** were identified as dicafeoyl quinic acid hexosides. Compounds **1**, **3** and **5** exhibited the same  $[M-H]^-$  ions at  $m/z$  677.19519, with a molecular formula of  $C_{28}H_{38}O_{19}$ . In the MS/MS spectra, their diagnostic ions at  $m/z$  353  $[CQA-H]^-$ ,  $m/z$  191  $[quinic\ acid-H]^-$  and  $m/z$  179  $[caffeic\ acid-H]^-$  indicated they were derivatives of CQA. Moreover, their fragmental ions at  $m/z$  515  $[M\text{-}C_6H_{10}O_5-H]^-$  and  $m/z$  353  $[M\text{-}C_6H_{10}O_5\text{-}C_6H_{10}O_5-H]^-$  indicated the existence of two hexosyl groups. Compounds **1**, **3**, and **5** were therefore identified as caffeoyl quinic acid hexosyl hexosides.

## 2.2. Simultaneous Quantification of 5-CQA, 4-CQA, 1,3-diCQA, 3,4-diCQA, 3,5-diCQA and 4,5-diCQA in Beagle Plasma after the Subcutaneous Injection of KZI

### 2.2.1. Optimization of HPLC-MS/MS Conditions for Quantitative Analysis

To quantify these six major caffeoyl quinic acids in beagle plasma, an XDB-C18 column using the optimized mobile phase was employed for sharp peak shapes with high intensity. The ion transition pairs were  $m/z$  value 353/191 for 5-CQA and 4-CQA;  $m/z$  value 515/353 for 1,3-diCQA, 3,4-diCQA, 3,5-diCQA and 4,5-diCQA; and  $m/z$  value 447/285 for astragalins, the internal standard. Optimized parameters are shown in Table 2. The major fragmentation of 5-CQA was the same as that of 4-CQA, and similar for 1,3-diCQA, 3,4-diCQA, 3,5-diCQA and 4,5-diCQA. In order to separate them in the shortest time with a satisfactory chromatographic resolution, the HPLC method was optimized (Section 3.3). The optimal retention times were 7.5, 8.7, 9.8, 14.0, 14.9, and 16.6 min for 5-CQA, 4-CQA, 1,3-diCQA, 3,4-diCQA, 3,5-diCQA and 4,5-diCQA, respectively.

**Table 2.** Optimized mass spectrometry conditions for 5-CQA, 4-CQA, 1,3-diCQA, 3,4-diCQA, 3,5-diCQA, and 4,5-diCQA and the internal standard, astragalin.

Analytes	Q1 Mass (Da)	Q3 Mass (Da)	DP (Volts)	EP (Volts)	CE (Volts)	CXP (Volts)
5-CQA	353	191	65	10	30	15
4-CQA	353	191	65	10	30	15
1,3-diCQA	515	353	85	10	27	15
3,4-diCQA	515	353	85	10	27	15
3,5-diCQA	515	353	85	10	27	15
4,5-diCQA	515	353	85	10	27	15
Internal standard	447	285	100	10	36	10

### 2.2.2. Method Validation

**Specificity.** Specificity was examined using blank beagle plasma and blank beagle plasma with added in 5-CQA, 4-CQA, 1,3-diCQA, 3,4-diCQA, 3,5-diCQA and 4,5-diCQA (each at 100.0 ng/mL) and the internal standard (100.0 ng/mL). No interference was found.

**Calibration curves and linearity.** Calibration curves were calculated using the peak area ratio of analytes compared with the internal standard. A weighting factor of  $1/X^2$  was used for linearity. The method demonstrated strong linear reliability. The six analytes showed linearity with concentration ranging from 6 to 600 ng/mL in beagle plasma. The lower limit of quantification (LLOQ) for 5-CQA, 4-CQA, 1,3-diCQA, 3,4-diCQA, 3,5-diCQA and 4,5-diCQA was 6 ng/mL.

**Accuracy and precision.** The quality control (QC) sample solutions were prepared in beagle plasma for 5-CQA, 4-CQA, 1,3-diCQA, 3,4-diCQA, 3,5-diCQA and 4,5-diCQA, each at 10, 100, and 400 ng/mL. Intra-day accuracy and precision were evaluated in six replicates of QC samples with different concentrations on the same day. Inter-day accuracy and precision were assessed in triplicates of QC samples with different concentrations on three days. Accuracy was calculated by comparing the mean concentration to the theoretical concentration. Precision was interpreted by the relative standard deviation (RSD). The intra-day and inter-day accuracy of six analytes at each concentration were in the range of 85–115%. The intra-day and inter-day precision of six analytes at each concentration were in the RSD range of 0–15%.

**Stability.** Long-term stability was evaluated in three replicates at different QC concentrations after storage at  $-80\text{ }^{\circ}\text{C}$  for 20 days. Freeze–thaw stability was assessed in three replicates of different QC concentrations after exposure to three sequential freeze–thaw cycles. For each cycle, samples were frozen for more than 24 h below  $-80\text{ }^{\circ}\text{C}$ , then transferred to a  $4\text{ }^{\circ}\text{C}$  environment for 2 h until completely thawed. Stability in an auto-sampler was evaluated in three replicates at different QC concentrations. Six analytes at each concentration were stable over 12 h in the auto-sampler. They were also stable after three freeze–thaw cycles and after 20 days of storage at  $-80\text{ }^{\circ}\text{C}$ .

### 2.2.3. Simultaneous Quantification of 5-CQA, 4-CQA, 1,3-diCQA, 3,4-diCQA, 3,5-diCQA and 4,5-diCQA in Beagle Plasma after the Subcutaneous Injection of KZI

The contents of 5-CQA, 4-CQA, 1,3-diCQA, 3,4-diCQA, 3,5-diCQA and 4,5-diCQA in KZI were determined as shown in Table 3. The quantitative HPLC-MS/MS method was applied to quantify 5-CQA, 4-CQA, 1,3-diCQA, 3,4-diCQA, 3,5-diCQA and 4,5-diCQA in beagle plasma samples. After the subcutaneous injection of KZI, beagle plasma exhibited quantifiable levels for all of the six analytes. As shown in Figure 4: At 0.5 h after the subcutaneous injection of KZI, 5-CQA reached the peak plasma concentration (61.23 ng/mL); 5 h after administration, the level of 5-CQA fell to under the LLOQ. At 0.25 h after the administration of KZI, 4-CQA reached the peak plasma concentration (114.87 ng/mL); 6 h after administration, the level of 4-CQA fell to under the LLOQ. At 0.5 h after administration of KZI, 1,3-diCQA reached the peak plasma concentration (11.20 ng/mL); 2.5 h after administration, the level of 1,3-diCQA fell to under the LLOQ. At 0.25 h after the



administration of KZI, 3,4-diCQA reached the peak plasma concentration (30.46 ng/mL); 2.5 h after administration, the level of 3,4-diCQA fell to under the LLOQ. At 0.25 h after administration of KZI, 3,5-diCQA reached the peak plasma concentration (19.49 ng/mL); 2 h after administration, the level of 3,5-diCQA fell to under the LLOQ. At 0.25 h after administration of KZI, 4,5-diCQA reached the peak plasma concentration (22.96 ng/mL); 2.5 h after administration, the level of 4,5-diCQA fell to under the LLOQ.

**Table 3.** Contents of 5-CQA, 4-CQA, 1,3-diCQA, 3,4-diCQA, 3,5-diCQA, and 4,5-diCQA in KZI.

Analytes	5-CQA	4-CQA	1,3-diCQA	3,4-diCQA	3,5-diCQA	4,5-diCQA
Contents ( $\mu\text{g/mL}$ )	46.2	48.0	9.7	190.0	11.7	17.2

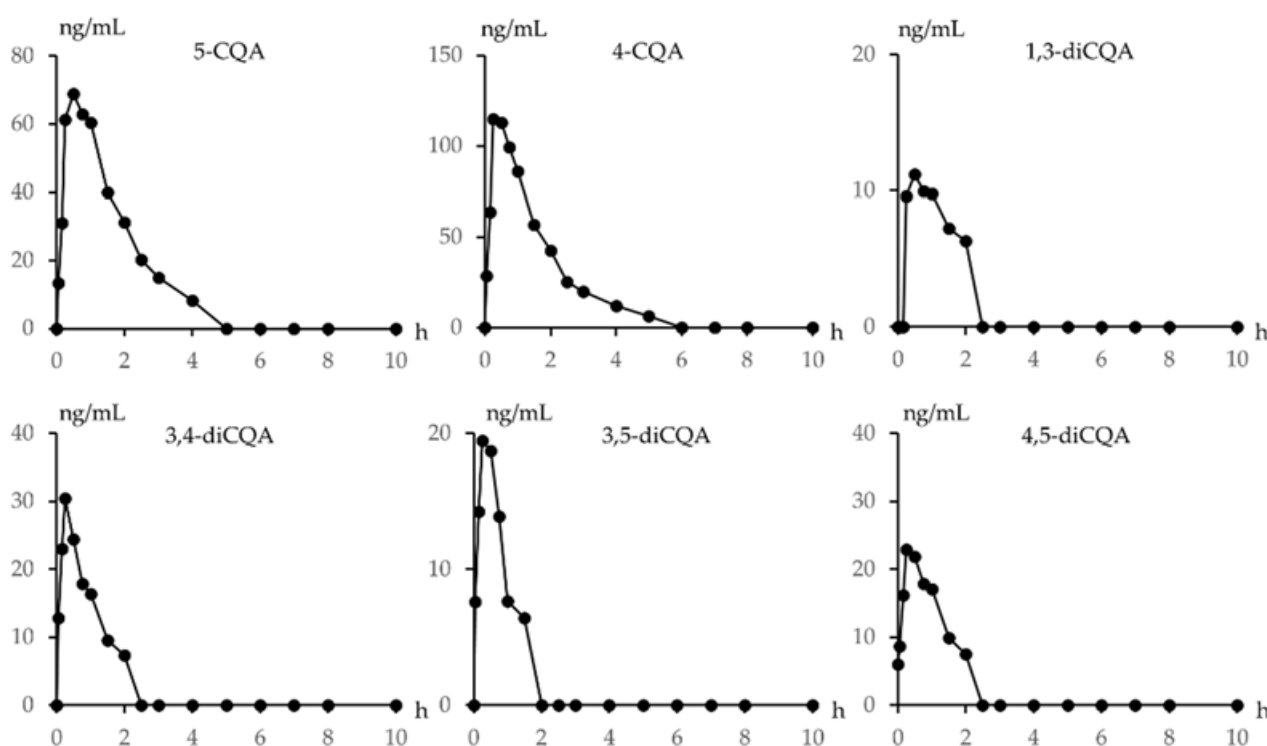


**Figure 4.** Concentration-time profiles of 5-CQA, 4-CQA, 1,3-diCQA, 3,4-diCQA, 3,5-diCQA, and 4,5-diCQA in beagle plasma after the subcutaneous injection of KZI.

### 3. Materials and Methods

#### 3.1. Materials

Reference standards of astragalins were purchased from MUST-Biological (Chengdu, China). 5-caffeoyl quinic acid, 4-caffeoyl quinic acid, 1,3-di-caffeoyl quinic acid, 3,4-di-caffeoyl quinic acid, 3,5-dicaffeoyl quinic acid and 4,5-dicaffeoyl quinic acid were provided by Xinjiang Technical Institute of Physics and Chemistry (Urumqi, China). Kaliziri Injections (Batch No. 190407) were purchased from Wuhu Yangyan Pharmaceutical Co., Ltd., (Wuhu, China). MS-grade methanol, acetonitrile and formic acid were purchased from Merck (Darmstadt, Germany) and Fisher Scientific (Fair Lawn, NJ, USA).

#### 3.2. UHPLC-Q-Orbitrap-MS Conditions

Qualitative analysis was performed on Q Exactive Orbitrap apparatus coupled with Ultimate 3000 equipment (Thermo Fisher Scientific, Waltham, MA, USA). The column was an HSS T<sub>3</sub> (1.8  $\mu\text{m}$ , 2.1  $\times$  100 mm, Waters, Ireland). The column oven temperature was 40 °C. The mobile solvents were A (acetonitrile, 0.1% *v/v* formic acid) and B (water, 0.1% *v/v* formic acid) with a flow rate of 250  $\mu\text{L}/\text{min}$  and in the following gradients:

0.0–2.0 min (0% A), 2.0–25.0 min (0–23% A), 25.0–40.0 min (23–83% A), 40.0–40.1 min (83–100% A), 40.1–45.0 min (100% A). The injected volume was 1  $\mu$ L. Electrospray ionization (ESI) was employed in positive mode and negative mode. The  $m/z$  range was 100–1200 with a resolution of 70,000. Voltage: 3.8 kV; sheath gas flow: 40 arb; auxiliary gas flow: 10 arb; heating temperature: 350  $^{\circ}$ C; capillary temperature: 350  $^{\circ}$ C; stepped normalized collision energy: 15, 40 and 65. The data were processed using the Xcalibur 4.2 software (Thermo Fisher Scientific, Waltham, MA, USA).

### 3.3. Quantitative HPLC-MS/MS Conditions

Quantitative HPLC-MS/MS analyses were performed using a 1200 system coupled with 4000 Q TRAP (Applied Biosystems/MDS Sciex, Framingham, MA, USA). The column was XDB-C18 (1.8  $\mu$ m, 4.6  $\times$  50 mm, Agilent, Santa Clara, CA, USA). The mobile solvents were A (acetonitrile, 0.2%  $v/v$  formic acid) and B (water, 0.2%  $v/v$  formic acid) with a flow rate of 0.6 mL/min and in the following gradients: 0.0–6.0 min (10–12% A), 6.0–6.1 min (12–20% A), 6.1–19.0 min (20–26% A). The injection volume was 10  $\mu$ L. The MS was in ESI-negative mode with multiple reaction monitoring (MRM). IonSpray voltage: –4000 V; nebulizer gas: 45; auxiliary heater gas: 55; curtain gas: 30; turbo gas temperature: 500  $^{\circ}$ C. The data were acquired with the Analyst 1.6.2 software (Applied Biosystems/MDS Sciex, Framingham, MA, USA) and processed with the MultiQuant 2.1 software (Applied Biosystems/MDS Sciex, Framingham, MA, USA).

### 3.4. Animal Experiment

Three male beagles were obtained from Xinjiang Medical University. They were fasted for 12 h before administration, but drank water freely. Animals were administrated subcutaneous KZI injection with a dose of 0.2 mL/kg. Blood was collected at 0, 0.05, 0.15, 0.25, 0.5, 0.75, 1, 1.5, 2, 2.5, 3, 4, 5, 6, 7, 8, and 10 h from hind limbs veins. Urine and feces were also collected. The collected blood was centrifuged for 15 min to produce plasma samples. The plasma samples were immediately stored at –80  $^{\circ}$ C.

### 3.5. Beagle Plasma Standard Solution Preparation

The stock solutions of 5-CQA, 4-CQA, 1,3-diCQA, 3,4-diCQA, 3,5-diCQA, 4,5-diCQA and the internal standard, astragaloside, were prepared by dissolving each compound in methanol to concentrations of 2.0 mg/mL and stored at –20  $^{\circ}$ C. Calibration curve standard sample preparation was as follows: 10  $\mu$ L appropriately diluted standard solutions (mixtures of 5-CQA, 4-CQA, 1,3-diCQA, 3,4-diCQA, 3,5-diCQA and 4,5-diCQA) was added into blank beagle plasma and vortexed for 10 s to result in samples containing 6–600 ng/mL standard compounds. The quality control (QC) sample solutions were prepared in beagle plasma for 5-CQA, 4-CQA, 1,3-diCQA, 3,4-diCQA, 3,5-diCQA and 4,5-diCQA, each at 10, 100, and 400 ng/mL.

### 3.6. Treatment of Beagle Plasma Samples

Beagle plasma samples were mixed with 10  $\mu$ L internal standard solution and vortexed for 10 s. Subsequently, 300  $\mu$ L acetonitrile was added and the mixture was vortexed for 60 s; then, it was centrifuged for 7 min. The supernatant was collected and nitrogen dried at 40  $^{\circ}$ C. The dried samples were mixed with 100  $\mu$ L methanol and sonicated for 60 s, then centrifuged for 7 min. The supernatant was collected and injected for analysis.

## 4. Conclusions

In this study, UHPLC-Q-Orbitrap-MS was employed to comprehensively characterize the caffeoyl quinic acid derivatives present in KZI. Based on accurate mass measurements, key fragmental ions and comparison with reference standards, 60 caffeoyl quinic acid derivatives were identified in KZI, including caffeoyl quinic acids, coumaroyl caffeoyl quinic acids, dicaffeoyl quinic acids, feruloyl caffeoyl quinic acids, dicaffeoyl quinic acid hexosides, etc. Moreover, an HPLC-MS/MS method was developed and validated for the

quantitative analysis of 5-CQA, 4-CQA, 1,3-diCQA, 3,4-diCQA, 3,5-diCQA and 4,5-diCQA in beagle plasma. The quantitative HPLC-MS/MS method was applied to quantify these six major caffeoyl quinic acids in beagle plasma after the subcutaneous injection of KZI. All of the six analytes reached their peak plasma concentration within 0.5 h. The 5-CQA and 4-CQA samples were quantifiable until a time point of 5 h. However, 1,3-diCQA, 3,4-diCQA, 3,5-diCQA and 4,5-diCQA fell under their LLOQs within 2.5 h.

**Author Contributions:** Conceptualization, H.A.A. and Y.L.; methodology, Liu, C.L. and A.W.; software, R.A.; validation, Y.L., C.L. and H.A.A.; formal analysis, X.L. and X.X.; investigation, C.L., A.W., J.D. and H.Z.; resources, X.L. and R.A.; data curation, A.W. and Y.L.; writing—original draft preparation, Y.L., X.X. and C.L.; writing—review and editing, Y.L. and H.A.A.; visualization, C.L. and A.W.; supervision, X.X. and Y.L.; project administration, Y.L. and C.L.; funding acquisition, H.A.A. All authors have read and agreed to the published version of the manuscript.

**Funding:** This work was supported by the National Key R&D Program of China under Grant 2020YFE020560.

**Institutional Review Board Statement:** The animal study protocol was approved by the Research Ethics Committee of Faculty of Medicine, Xinjiang Medical University, China (Approval code: IACUC-20200924-29; Date of approval: 24 September 2020).

**Informed Consent Statement:** Not applicable.

**Data Availability Statement:** Data sharing not applicable.

**Conflicts of Interest:** The authors declare no conflict of interest.

## References

1. Ezzedine, K.; Lim, H.W.; Suzuki, T.; Katayama, I.; Hamzavi, I.; Lan, C.C.E.; Goh, B.K.; Anbar, T.; Castro, C.S.; Lee, A.Y.; et al. Revised classification/nomenclature of vitiligo and related issues: The vitiligo global issues consensus conference. *Pigm. Cell Melanoma R.* **2012**, *25*, E1–E13. [[CrossRef](#)] [[PubMed](#)]
2. Boniface, K.; Seneschal, J. Vitiligo as a skin memory disease: The need for early intervention with immunomodulating agents and a maintenance therapy to target resident memory T cells. *Exp. Dermatol.* **2019**, *28*, 656–661. [[CrossRef](#)] [[PubMed](#)]
3. Zhang, X.J.; Liu, J.B.; Gui, J.P.; Li, M.; Xiong, Q.G.; Wu, H.B.; Li, J.X.; Yang, S.; Wang, H.Y.; Gao, M.; et al. Characteristics of genetic epidemiology and genetic models for vitiligo. *J. Am. Acad. Dermatol.* **2004**, *51*, 383–390. [[CrossRef](#)] [[PubMed](#)]
4. Taieb, A.; Alomar, A.; Boehm, M.; Dell’Anna, M.L.; De Pase, A.; Eleftheriadou, V.; Ezzedine, K.; Gauthier, Y.; Gawkrödger, D.J.; Jouary, T.; et al. Guidelines for the management of vitiligo: The european dermatology forum consensus. *Br. J. Dermatol.* **2013**, *168*, 5–19. [[CrossRef](#)] [[PubMed](#)]
5. Kostopoulou, P.; Jouary, T.; Quintard, B.; Ezzedine, K.; Marques, S.; Boutchnei, S.; Taieb, A. Objective Vs. subjective factors in the psychological impact of vitiligo: The experience from a french referral centre. *Br. J. Dermatol.* **2009**, *161*, 128–133. [[CrossRef](#)] [[PubMed](#)]
6. Homan, M.W.L.; de Korte, J.; Grootenhuis, M.A.; Bos, J.D.; Sprangers, M.A.G.; van der Veen, J.P.W. Impact of childhood vitiligo on adult life. *Br. J. Dermatol.* **2008**, *159*, 915–920. [[CrossRef](#)] [[PubMed](#)]
7. Dogra, N.K.; Kumar, S.; Kumar, D. *Vernonia anthelmintica* (L.) Willd.: An ethnomedicinal, phytochemical, pharmacological and toxicological review. *J. Ethnopharmacol.* **2020**, *256*, 112777. [[CrossRef](#)]
8. Turak, A.; Liu, Y.Q.; Aisa, H.A. Elemanolide dimers from seeds of *Vernonia anthelmintica*. *Fitoterapia* **2015**, *104*, 23–30. [[CrossRef](#)]
9. Wang, J.Y.; Luo, L.; Ding, Q.; Wu, Z.R.; Peng, Y.Y.; Li, J.; Wang, X.Q.; Li, W.H.; Liu, G.X.; Zhang, B.; et al. Development of a multi-target strategy for the treatment of vitiligo via machine learning and network analysis methods. *Front. Pharmacol.* **2021**, *12*, 754175. [[CrossRef](#)]
10. Lai, Y.F.; Feng, Q.Y.; Zhang, R.; Shang, J.; Zhong, H. The great capacity on promoting melanogenesis of three compatible components in *Vernonia anthelmintica* (L.) Willd. *Int. J. Mol. Sci.* **2021**, *22*, 4073. [[CrossRef](#)]
11. Rajan, M.; Feba, K.S.; Chandran, V.; Shahena, S.; Mathew, L. Enhancement of rhamnetin production in *Vernonia anthelmintica* (L.) Willd. cell suspension cultures by eliciting with methyl jasmonate and salicylic acid. *Physiol. Mol. Biol. Pla.* **2020**, *26*, 1531–1539. [[CrossRef](#)] [[PubMed](#)]
12. Wang, Q.; Wang, Y.X.; Pang, S.L.; Zhou, J.; Cai, J.; Shang, J. Alcohol extract from *Vernonia anthelmintica* (L.) willd. seed counteracts stress-induced murine hair follicle growth inhibition. *BMC Complem. Altern. Med.* **2019**, *19*, 372. [[CrossRef](#)] [[PubMed](#)]
13. Huo, S.X.; Wang, Q.; Liu, X.M.; Ge, C.H.; Gao, L.; Peng, X.M.; Yan, M. The effect of butin on the vitiligo mouse model induced by hydroquinone. *Phytother. Res.* **2017**, *31*, 740–746. [[CrossRef](#)] [[PubMed](#)]
14. Zhou, J.; Shang, J.; Ping, F.F.; Zhao, G.R. Alcohol extract from *Vernonia anthelmintica* (L.) willd. seed enhances melanin synthesis through activation of the p38 MAPK signaling pathway in B16F10 cells and primary melanocytes. *J. Ethnopharmacol.* **2012**, *143*, 639–647. [[CrossRef](#)]

15. Wu, B.; Zhu, Y.J.; Wa, Q.B.; Liu, L.; Gu, L.Q. Efficacy of 308 nm excimer laser plus *Vernonia anthelmintica* willd. injection in 60 cases of vitiligo. *Chin. J. Derm. Venereol.* **2014**, *28*, 1209–1210.
16. Sun, H.M.; Xu, Z.T. Efficacy of *Vernonia anthelmintica* injection combined with vitiligo pill in the treatment of vitiligo. *World Latest Med. Inform.* **2015**, *15*, 185–188.
17. Deng, R.C.; Zhou, Y.; Zhang, W.S.; Xu, J.G.; Shang, J.; Wang, X.D.; Yu, L.H. Study on mechanism of vitiligo by *Vernonia anthelmintica* Willd. *Lett. Biotech.* **2004**, *15*, 573–576.
18. Zhao, Y.; Lu, H.; Wang, Q.; Liu, H.; Shen, H.; Xu, W.; Ge, J.; He, D. Rapid qualitative profiling and quantitative analysis of phenolics in *Ribes meyeri* leaves and their antioxidant and antidiabetic activities by HPLC-QTOF-MS/MS and UHPLC-MS/MS. *J. Sep. Sci.* **2021**, *44*, 1404–1420. [[CrossRef](#)]
19. Ersan, S.; Ustundag, O.G.; Carle, R.; Schweiggert, R.M. Identification of phenolic compounds in red and green pistachio (*Pistacia vera* L.) hulls (Exo- and Mesocarp) by HPLC-DAD-ESI-(HR)-MS<sup>n</sup>. *J. Agri. Food Chem.* **2016**, *64*, 5334–5344. [[CrossRef](#)]
20. Gouveia, S.C.; Castilho, P.C. Characterization of phenolic compounds in *Helichrysum melaleucum* by high-performance liquid chromatography with on-line ultraviolet and mass spectrometry detection. *Rapid Commun. Mass Spectrom.* **2010**, *24*, 1851–1868. [[CrossRef](#)]
21. Ammar, S.; Contreras, M.D.; Gargouri, B.; Segura-Carretero, A.; Bouaziz, M. RP-HPLC-DAD-ESI-QTOF-MS based metabolic profiling of the potential *Olea europaea* by-product “wood” and its comparison with leaf counterpart. *Phytochem. Anal.* **2017**, *28*, 217–229. [[CrossRef](#)] [[PubMed](#)]
22. Sommella, E.; Pagano, F.; Salviati, E.; Chieppa, M.; Bertamino, A.; Manfra, M.; Sala, M.; Novellino, E.; Campiglia, P. Chemical profiling of bioactive constituents in hop cones and pellets extracts by online comprehensive two-dimensional liquid chromatography with tandem mass spectrometry and direct infusion Fourier transform ion cyclotron resonance mass spectrometry. *J. Sep. Sci.* **2018**, *41*, 1548–1557. [[CrossRef](#)] [[PubMed](#)]
23. Sollicec, M.; Roy-Lachapelle, A.; Sauve, S. Quantitative performance of liquid chromatography coupled to Q-Exactive high resolution mass spectrometry (HRMS) for the analysis of tetracyclines in a complex matrix. *Anal. Chim. Acta* **2015**, *853*, 415–424. [[CrossRef](#)] [[PubMed](#)]